Chapter 1

Manipulation of Tribological Properties of Metals by Ultrashort Pulsed Laser Micro-/Nanostructuring

Quan-Zhong Zhao and Zhuo Wang

Additional information is available at the end of the chapter

http://dx.doi.org/10.5772/64764

Abstract

Surface texturing as a means for controlling tribological properties of mechanical components is well known for many years. Various technologies have been developed for surface texturing. Among them, ultrashort pulsed laser surface texturing is one of the most promising ways to achieve micromachining in the field of tribological applications. Ultrashort pulsed laser technology can produce various micro-/nanostructures on the material surfaces to modulate their tribological properties. The aim of this chapter is to introduce the recent progress on ultrashort pulsed laser-induced frictional property change of metals and to demonstrate the potential applications of ultrashort pulsed laser-induced frictional property change of metal in various fields.

Keywords: ultrashort pulsed laser micro-/nanostructuring, surface texturing, tribological property, metals

1. Introduction

In the past decades, there has been a growing interest in the designing of surface structures in micro-/nanoscale to modulate tribological properties of materials [1–3]. Various surface modification technologies have been proposed to tune the tribological properties of various materials [1–3]. Surface texturing, an artificial topography on the surface of material, has been introduced to modulate the tribological properties of materials [1]. These textured surfaces can act as lubricant reservoirs for supplying lubricant, as traps for wear debris, and as microhydrodynamic bearings for improving load-carrying capacity [4–8]. Up till now, these textured surfaces have been utilized to improve the tribological performances of interfaces in various fields, such as piston rings, mechanical seals, thrust bearing, magnetic storage devices, cutting tools, and microelectro-mechanical system (MEMS) [9–14].

Many surface texturing technologies, including mechanical processing, lithography, ion beam texturing, and laser surface texturing have been developed for producing the micro-/nanometer-sized structures on different material surfaces [15–18]. Compared to other techniques, laser structuring provides significant advantages including fast machining time, environment friendly, precise control of the geometric features of the patterns, and so on. Especially, the ultrashort pulsed laser with pulse width ranging from picosecond to femtosecond is one of the most promising ways to achieve micromachining in the field of tribological applications [19–37], which is owing to its ultrashort pulse width and ultrahigh peak power that can process almost all materials. Moreover, ultrashort pulsed lasers are expected to minimize the melt ejection and heat-affected effects for surface texturing in tribological applications.

Some researchers have proved that ultrashort pulsed laser structuring can modulate the friction behaviors of metal materials [23–37]. Surface textures not only reduce the friction coefficient, but also can raise the friction coefficient, depending on the geometry, scale, and subsequent modification. The aim of this chapter is to introduce the recent progress on ultrashort pulsed laser-induced frictional property change of metals and to demonstrate the potential applications of ultrashort pulsed laser-induced frictional property change of metal in various fields.

2. Ultrashort pulsed laser-induced micro-/nanostructures on the surface of metals: phenomena and mechanisms

Laser surface modification has been intensively studied since the invention of laser. The first step in any structural modification of a material by laser processing is the deposition of laser energy. The total laser energy and the spatial and temporal energy distribution determine what kind of final structure on the modified surface will be obtained [38].

During the interaction of laser pulses with metal targets, the laser energy is absorbed by free electrons through such mechanisms as inverse bremsstrahlung [39]. Then the evolution is the excitation of electrons from their equilibrium states to excited states by absorbing photons. The electronic excitation is followed by multiple secondary processes, ultimately ending in the final structural modification of the material. The time scales of various secondary processes can be identified as shown in **Figure 1** [38].

The primary electronic excitation is related to a quite short-lived coherent polarization of the metal material. The polarization is destroyed during the dephasing process within a time scale of about 10^{-14} s [40]. The pure dephasing changes the phase of the excited states but have no effect on the electronic energy distribution. The started distribution of excited electronic states corresponds to the set of states coupled by the optical transitions. The occupation of these primary states is promptly changed by the process of carrier-carrier interaction, and a quasi-equilibrium state is established among the electrons within a time scale of approximately

10^{-13}s. At this moment, the electron temperature (T_e) is greater than the lattice temperature (T_i). Subsequently, the quasi-equilibrium electrons cool down on a time scale of 10^{-13}–10^{-12} s by emission of phonons. The final stage of the thermalization process is the redistribution of the phonons over the entire Brillouin zone according to a Bose-Einstein distribution. It is generally accepted that a few picoseconds after the deposition of the laser energy the energy distribution is close enough to the thermal equilibrium. The thermal diffusion can take place on a time scale of the order of 10^{-11} s after the thermalization. The solid-liquid transition will take place at melting temperature when a sufficient amount of energy is deposited in the metal.

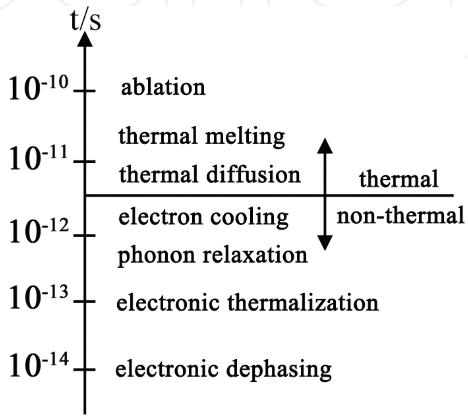

Figure 1. Time scale of the various secondary processes [38].

As mentioned above, it can be concluded that a distinct dividing line at about 10^{-12} s separate the regime of nonthermal processes and thermal processes. For the pulsed laser-metal interaction process, if the pulse duration (pulse width) is much longer than 10^{-12}s, the whole process will involve thermalization within the electron subsystem, energy transfer to the lattice, and energy losses due to the electron heat transport into target. Thus, the thermal mechanisms of laser ablation such as melting and boiling are likely to play an important role. While if the pulse duration is much shorter than 10^{-12}s, the thermal diffusion can be neglected, which avoids negative effects of energy transfer.

Chichkov et al. [41] compared holes drilled in 100 μm thick steel foils (in vacuum) with a pulse duration of 3.3 ns (1 ns = 10^{-9}s) laser and a pulse duration of 200 fs (1 fs = 10^{-15}s) laser. **Figure 2(a)** and **(c)** shows the schematic of nanosecond-pulse ablation and the surface morphology of holes drilled with a pulse duration of 3.3 ns and a fluence of F = 4.2 J/cm². The trace of the molten material can be seen in **Figure 2(c)**. Due to the longer pulse duration of nanosecond pulses, there is enough time for the thermal wave to propagate into the metal target and to create a relatively large molten layer. Thus, the solid-liquid and solid-vapor transformation take place in the process of laser ablation. The molten material is pushed out by the recoil pressure produced by the vaporization process, which lead to a "corona" around the hole as shown in **Figure 2(c)**. **Figure 2(b)** and **(d)** presents the schematic of femtosecond-pulse laser ablation and the hole drilled with a duration of 200 fs and a fluence of F = 0.5 J/cm². It can be seen that there is no trace of the molten material and only a vapor dust ring around the hole. As mentioned above, when the laser pulse duration is much shorter than time scale of thermal diffusion, nonthermal ablation mechanisms will occur. Due to the very short time scales involved in the ablation with femtosecond laser pulses, direct ionization and the formation of dense electron-hole plasmas can result in athermal phase transition, direct bond breaking, and explosive disintegration of the lattice through electronic repulsion. Therefore, the thermal conduction into metal can be neglected.

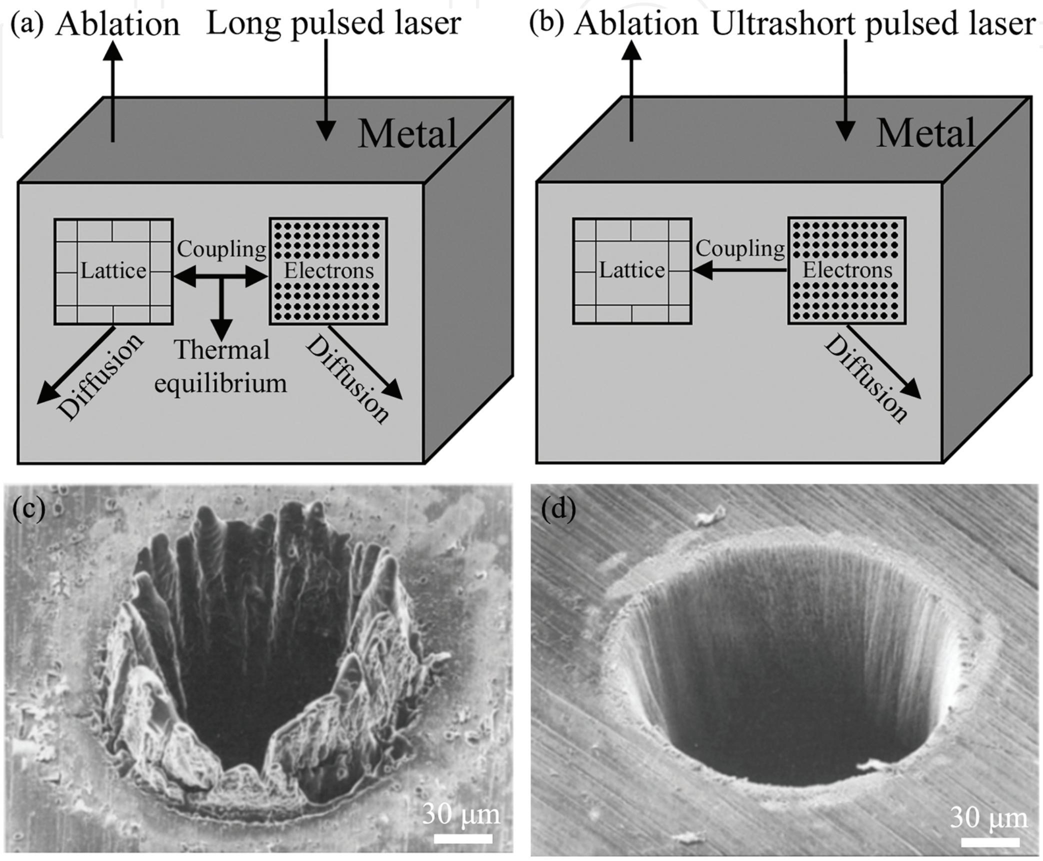

Figure 2. Schematic of nanosecond/femtosecond-pulse laser ablation and surface morphology of holes drilled in a 100 μm thick steel foil. (a) Schematic of nanosecond-pulse laser ablation, (b) schematic of femtosecond-pulse laser ablation, (c) surface morphology of holes drilled through a steel foil with a pulse duration of 3.3 ns and a fluence of $F = 4.2$ J/cm^2, (d) surface morphology of holes drilled through a steel foil with a pulse duration of 200 fs and a fluence of $F = 0.5$ J/cm^2 [41].

As early as 1965, a kind of near-wavelength periodic structures has been discovered in optical damages on semiconductor surfaces induced by a ruby laser [42]. Since then, these laser-induced periodic surface structures (LIPSS) or the so-called ripples have been studied extensively on various material surfaces. Recently, LIPSS as a kind of nanostructures have gained remarkable interest because they enable tuning of a wide range of properties, including wettability, colorization, and tribological properties [43–45]. In this section, we will introduce phenomena and mechanisms concerning ultrashort pulsed laser-induced periodic surface structures on the surface of metals.

Ultrashort pulsed laser-induced ripples on the surface of metals are formed as a result of light-matter interaction and their period (Λ), orientation, and morphology are strongly dependent

http://dx.doi.org/10.5772/64764

on both the material properties and the laser irradiation conditions, including polarization, angles of incidence, laser energy fluence, incident light wavelength (λ), and pulse number/ scanning speed [46–49]. Period is the most important ripples' parameter. Nowadays, ultrashort pulsed laser can easily induce subwavelength ripples on different metals. In general, the ripples can be separated into near-subwavelength ripples (NSRs, $0.4 < \Lambda/\lambda < 1$) and deep-subwavelength ripples (DSRs, $\Lambda/\lambda < 0.4$) in normal incidence [48, 50]. Orientation of ripples with respect to irradiation polarization is another parameter allowing to distinguish different ripple morphologies. For a linearly polarized laser beam, the origination of ripples is most often perpendicular to the incident laser polarization [51]. **Figure 3** shows uniform periodic nanostructures produced on the surface of stainless steel using an 800-nm femtosecond laser. It can be seen that the ripples are oriented perpendicular to the incident laser polarization (white double arrows direction). The period in the ripple structures is measured to be about 560 nm along the polarization direction, which is less than the wavelength of the employed femtosecond laser.

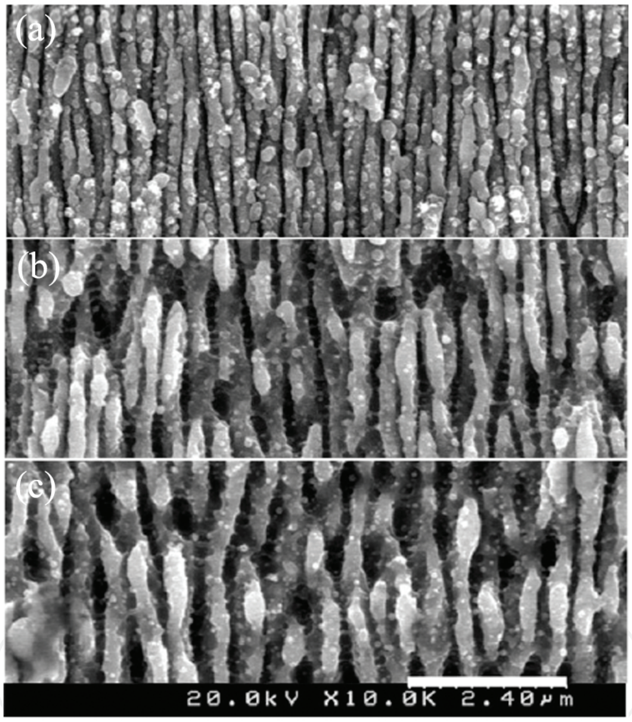

Figure 3. SEM images of the 304 stainless steel surfaces ablated by an 800-nm femtosecond laser. (a) DSRs, (b) NSRs, and (c) NSRs [48].

However, early studies showed that the period of ripples (Λ) is close to the incident light wavelength (λ) with a strong dependence on the angle of incidence (θ) when the ripples formed on the surface of metals using lasers with long pulse width (≥ns) [52].

$$\Lambda = \frac{\lambda}{1 \pm \sin\theta} \tag{1}$$

where the sign + or − depends on a scattered wave direction toward (+) or from (−) the incident beam. These classical ripples are widely accepted as a result of the interaction between the incident light and the surface scattering wave [52–54]. However, the period of ripple is generally found smaller compared to the laser wavelength when the ripple induced by using ultrashort pulsed lasers such as femtosecond lasers. Thus, the subwavelength ripples should not be ascribed to the classical ripples described by the scattering mode. Recently, some researchers propose that the interaction between the incident laser light and the excited surface plasma (SP) wave is responsible for the formation of ripples induced by femtosecond pulsed lasers on a metal surface [50]. They believed that the propagating SPs and the incident laser will interfere to form a fringe with a vector as shown in **Figure 4**:

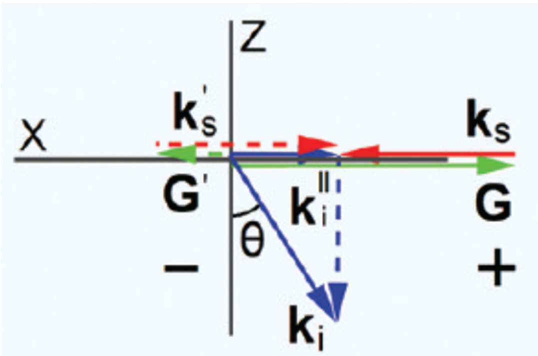

Figure 4. Schematic processes of SP-laser interactions [50].

$$\mathbf{G} = \mathbf{k}_i - \mathbf{k}_s \tag{2}$$

where $\mathbf{k}_i$ is the wavevector of incident laser, and $\mathbf{k}_s$ is the wavevector of SPs. Considering the components in the interface, they obtain

$$\Lambda = \frac{\lambda}{\frac{\lambda}{\lambda s} \pm \sin\theta} \tag{3}$$

where $\Lambda = 2\pi\ |\mathbf{G}|^{-1}$, $\lambda = 2\pi\ |\mathbf{k}_i|^{-1}$, $\lambda_s = 2\pi\ |\mathbf{k}_s|^{-1}$, and θ is the incident angle of laser. Assume $\varepsilon'' < |\varepsilon'|$ (ε'' is the imaginary part of ε), the λ_s on a metal/dielectric interface is given by Raether [55]

$$\lambda_s = \lambda\left(\frac{\varepsilon' + \varepsilon_d}{\varepsilon'\varepsilon_d}\right)^{1/2} \tag{4}$$

where ε_d is the dielectric constant of the dielectric material (for air, $\varepsilon_d \approx 1$). Thus, the simple relationship $\Lambda = \lambda_s$ can be obtained in normal incidence. It means that in the situation with a destructible fluence, the interference fringes will induce permanent ripples on material surface with Λ equal to λ_s, which is always smaller than λ.

3. Modulation of tribological property of metals by ultrashort pulsed laser-induced microstructures

Lasers with long pulse width are used to produce surface textures to improve tribological properties of metal in the early stage [9, 11]. However, there is an obvious thermal effect during the long pulse width laser ablation process, which results in the reduction of machining accuracy. As above-mentioned, the ultrashort pulsed lasers, owing to their ultrashort pulse width and ultrahigh peak power, can safely process almost all materials with minimal heat effects for surface texturing. Therefore, the ultrashort pulsed laser surface texturing is expected to be a useful tool for improving tribological properties of materials (**Figure 5**).

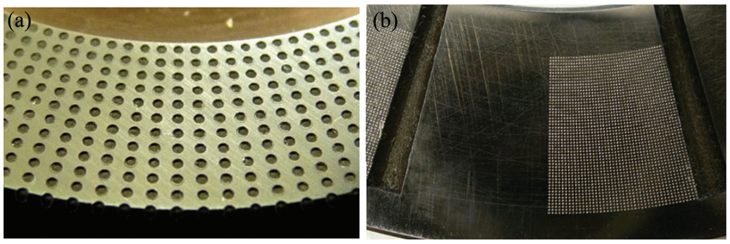

Figure 5. Laser textured surface. (a) Laser-textured stationary specimen of the seal. (b) Laser-textured thrust bearing [9, 11].

As early as 2004, Dumitru et al. [25] studied the effect of femtosecond laser ablation on tribological properties of coated WC-Co surfaces under dry condition. Surface textures with various shapes were found to occur after a given number of incident femtosecond laser pulses and the tribological tests demonstrated improved wear behaviors for the patterned coated WC-Co surfaces. **Figure 6** showed that the particle trap role of the femtosecond laser-induced pores is responsible for the improvement of tribological properties of coated WC-Co surfaces to a great extent.

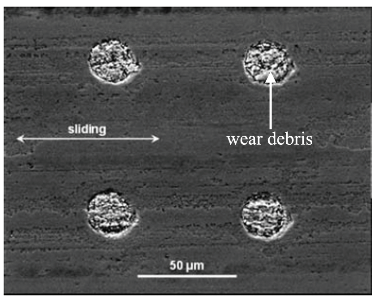

Figure 6. SEM image from wear track of the patterned coated WC-Co surface [25].

As mentioned above, ultrashort pulsed laser technology is one of the most promising ways to achieve micromachining in the field of tribological applications. In comparison of other laser-textured surface, there is very minimal resolidified and spatter particles on the ultrashort pulsed laser-textured surface due to its ablation mechanism. Bathe et al. [26] investigated the effect of laser-textured surface produced by different laser sources on the tribological behavior of gray cast iron under dry condition. The microtextured surfaces with dimple feature were produced on gray cast iron using millisecond (0.5 ms), nanosecond (40 ns), and femtosecond (120 fs) laser source. As shown in **Figure 7**, the femtosecond laser-textured surface exhibited the lowest steady-state coefficient and wear rate among the tested samples. The reason is ascribed to the absence or very minimal resolidified particles present on femtosecond laser-textured surface. During sliding wear test, the resolidified and spatter particles on the metal surface is collapsed readily, which is generally detrimental to the tribological properties. Moreover, the dimple can capture wear debris and reduce the plowing of metal surface. Consequently, the femtosecond laser-textured surfaces show a considerable lower friction coefficient and wear rates compared with the untextured and other long pulse width laser-textured surfaces. The SEM images of the wear track of the textured and untextured samples are shown in **Figure 8**. It can be seen that a spread of wear debris cover the worn surface of the untextured samples (**Figure 8a**). However, the wear track does not show much wear debris on surface (**Figure 8b–d**). This indicates that wear debris moves from the contact region and fills the dimples. In this case, dimples act as reservoirs of debris that leave free interface between the friction pairs, thus reducing friction and wear.

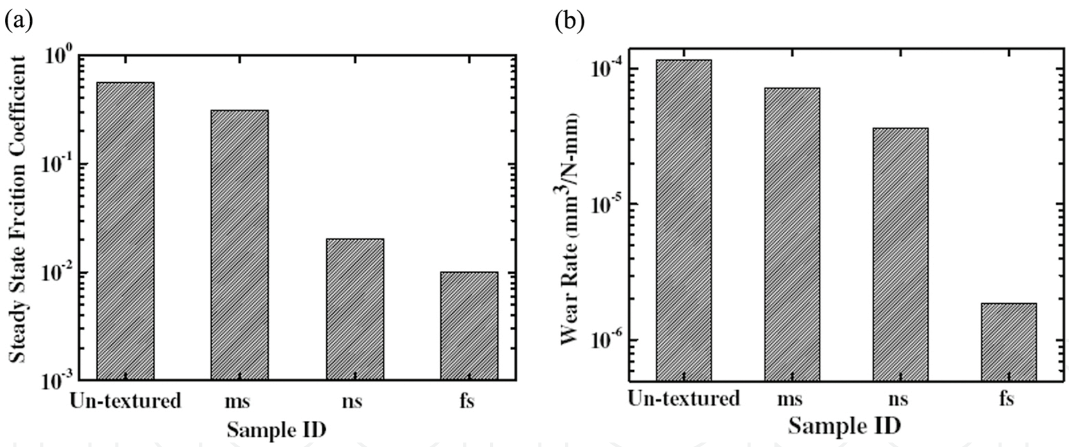

Figure 7. Ball-on-disk test performed at room temperature: (a) steady-state friction coefficient for untextured and textured samples, (b) wear rate for untextured and textured samples [26].

Femtosecond laser surface texturing not only reduces the friction coefficient, but also can raise the friction coefficient. The authors of this chapter have [27] found that tribological property of textured surfaces by femtosecond laser can be modulated. By producing regular arranged microgrooved textures with different spacing on the AISI 304L steel surfaces by an 800-nm femtosecond laser, they proved that the spacing of microgrooves had a significant impact on friction coefficient of textured surfaces under dry condition. As the spacing of the textured surfaces increases, the average friction coefficients first decrease and then increase (**Figure 9**).

And the structured surface with a microgroove spacing of 100 μm has the minimal average friction coefficient. When the period of microgroove is within 15–35 μm, the average friction coefficients of structured surfaces are more than that of the unstructured surface. However, when the period of microgroove is in the range of 50–300 μm, the average friction coefficients of structured surfaces are smaller than that of unstructured surface. In conclusion, the increase or decrease of average friction coefficient of textures surfaces depends on the microgroove spacing compared with untextured surface.

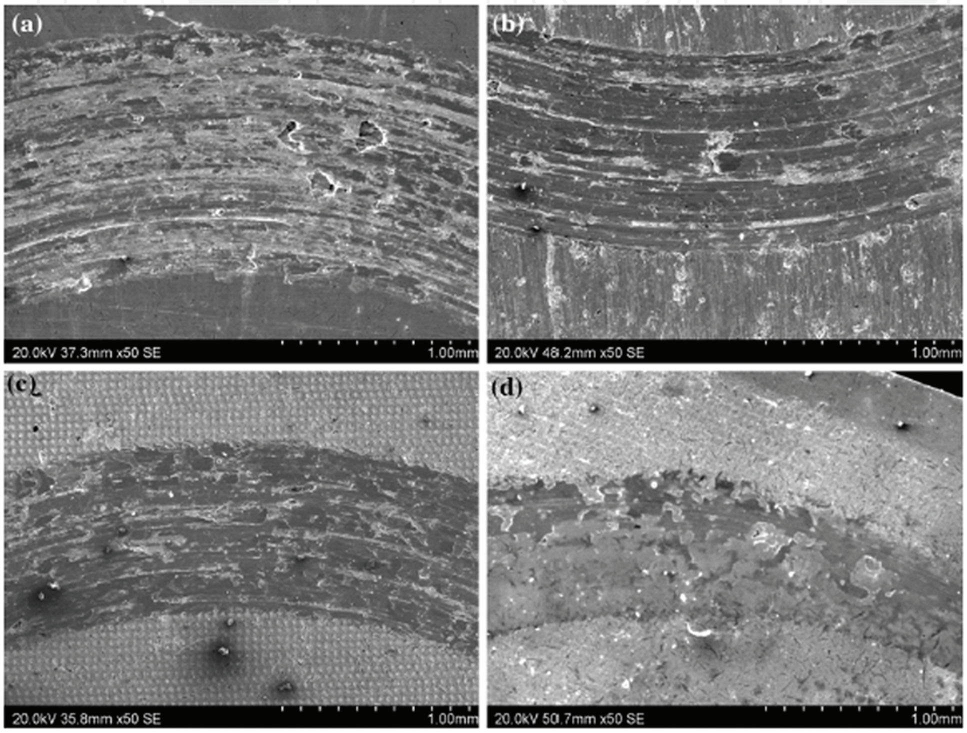

Figure 8. SEM images of wear track of (a) untextured, (b) millisecond laser textured, (c) nanosecond laser textured, and (d) femtosecond laser-textured samples [26].

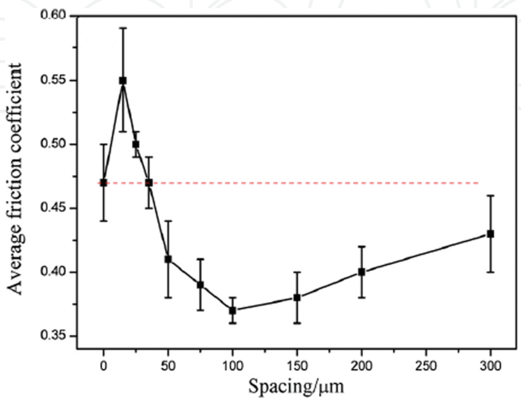

Figure 9. Average friction coefficients of untextured surface and textured surfaces with different microgroove spacing [27].

The result can be ascribed to the changing contributions of the three components of friction, i.e., due to the adhesion, to the plowing, and to the deformation [56]. The friction coefficient can be formulated by Eq. (5) under dry condition:

$$\mu = \mu_a + \mu_p + \mu_d \tag{5}$$

where μ_a is the adhesion friction coefficient component which is related to the real contact area [57], μ_p is the plowing friction coefficient component which is related to wear debris, and μ_d is the deformation friction coefficient component which is related to the surface roughness and contact stress, respectively [58]. As the increase of spacing of textured surfaces, the density of microgrooved textures decreases and the real contact area between two relative sliding surfaces increases correspondingly. The adhesion friction coefficient component depends on the real area of contact [57]. So, when the real area of contact increases, adhesion friction coefficient component increases. The plowing friction coefficient component also increases with the period of the microgroove as to the trapped effect becomes weaker. While the deformation component of friction coefficient decrease with the increase of spacing of textured surfaces due to the decrease of the contact stress. The small real contact corresponding to large contact stress may result in a transition from elastic deformation to the plastic deformation, usually causing a great increase of the friction force. Meanwhile, the deformation and collision of asperities lead to the ratchet coefficient which depends on the surface roughness. With increasing the period of microgrooves, the roughness of textured surfaces reduces, accordingly, the deformation friction coefficient component decreases. Therefore, there is a minimal friction coefficient caused by the changing contributions of three friction components. In summary, friction coefficients of AISI 304L steel can be controlled by changing the period of microgrooves of the textured surfaces.

Ultrashort pulsed laser surface texturing can reduce friction and wear under lubrication condition as well. In metal cutting with continuous chips, severe friction exists as the chip flows over the rake face of the cutting tool at high normal load and speed. In order to reduce friction and wear between the chip and the tool rake face, Lei et al. [28] utilized femtosecond laser surface texturing to produce microholes to form micropools filled with liquid or solid lubricants on the rake face of WC cutting inserts. They conducted a comparative investigation between micropool lubricated (surface-textured) cutting tools and flood-cooled (untextured) cutting tools. The cutting tests showed that the friction coefficient of the textured surface significantly reduced compared with that of untextured surface. The following two mechanisms can explain this phenomenon. First, the direct chip-tool contact area was reduced with embedded micropools that contain liquid or solid lubricants. Second, the lubricant may be squeezed out or spread over by the rubbing action of the chip flowing over the micropools to form a thin film at the chip-tool interface thus direct chip-tool contact can be further reduced. Consequently, the smaller direct contact area between the chip and tool rake face leaded to less friction coefficient. Ling et al. [29] also reported a research on utilization of surface textures to reduce adhesion and enhance drill bit life. The results from this study reveal that surface textures induced by picosecond laser on the margins of drill bits is a promising method for these purposes. The surface textures can serve as microreservoirs to retain some lubricant and release it under pressure or physical scribing. Therefore, properly designed microscale surface textures could provide positive impact on lubrication enhancement.

Surface texture will inevitably cause an increase in surface roughness which may destroy the oil films due to large local contact stress. Thus, a critical issue in application of surface texturing concerns the optimum surface texture under lubrication condition. The authors of this chapter [30] have investigated the effect of femtosecond laser-induced microgrooves on starved lubrication tribological properties of stainless steel. The results show that the average friction coefficients initially decrease and then increase as the spacing of the textured surfaces increases. Moreover, the average friction coefficient of textured surface is reduced by 30.9% with their optimum microgroove spacing (75 μm) compared with that of untextured surface. When the period of microgroove is very small, the reduction of actual contact area between friction pairs enhances the average contact stress at the sliding surface, which makes the oil film easily collapsible in the untreated region. When the period of microgroove is very large, the grooves as oil reservoirs (secondary lubrication effect) cannot be sufficiently provided to the sliding contact surface, and the wear debris cannot be effectively trapped by the grooves (wear debris-trapped effect). Therefore, the changing contributions of the three effects of friction lead to the existence of the optimum friction property for the textured samples with the increase of microgroove spacing. In a word, femtosecond laser surface texturing has a marked potential for reducing friction and wear under lubrication condition if the surface textures were distributed in an appropriate manner.

4. Reduction of friction of metals by ultrashort pulsed laser-induced periodic surface nanostructures

Laser-induced periodic surface structures (LIPSS) or the so-called ripple structures exhibit several amazing properties such as the capability of tuning wettability, reflectivity, and tribological properties. The modification of tribological properties has specifically attracted attention because of its potential application in industrial fields such as magnetic recording devices, cutting tools, and microelectro-mechanical system (MEMS) [12–14].

As the density of magnetic recording on computer hard disk drive increases rapidly and approaches the level of 1 Tb/in^2, the flying height of the magnetic head (the slider), or hard disk interface, has to be reduced to about 5 nm. Such ultralow hard disk interface can only be realized on super smooth surfaces of slider and disk; however, this will result in serious stiction at the hard disk interfaces. Therefore, reduction of the interfacial adhesion and stiction has attracted great attentions in recent years. Some researchers found that the surface texturing is an effective method to reduce stiction and adhesion at the hard disk interfaces. Hanchi et al. [59] reported that the textured sliders can prevent the catastrophic failure caused by a sudden rise of friction from super smooth surface. Wang et al. [60] also showed that the textured sliders exhibited less lubricant depletion and smaller vibrations compared with untextured sliders. Tagawa et al. [31] proposed a novel concept of contact sliders with nanotextures produced by femtosecond laser processing. Contact sliders experiments were carried out using the contact sliders with and without nanotextures. It was found that the nanotextured sliders facilitate the development of contact hard disk interface with lower friction, low wear of the contact slider surfaces, and low contact sliders bouncing vibration.

One of the successful applications of laser surface texturing is in cutting tools. Surface textures with micrometer scales on the tool surface have been reported to improve tribological characteristics [32, 33]. The nanoscale textures are also the ideal candidate for improving the properties of cutting tools. Kawasegi et al. [32] developed WC-Co cutting tools that had nanoscale textures on their surfaces using interference inscription of a femtosecond laser. The effect of nanoscale textures on the machinability of an aluminum alloy was investigated with a turning experiment applying the minimum quantity lubrication method. The tested results indicated that the ripple structure decreased the cutting force due to the corresponding reduction in the friction on the rake face (**Figure 10**).

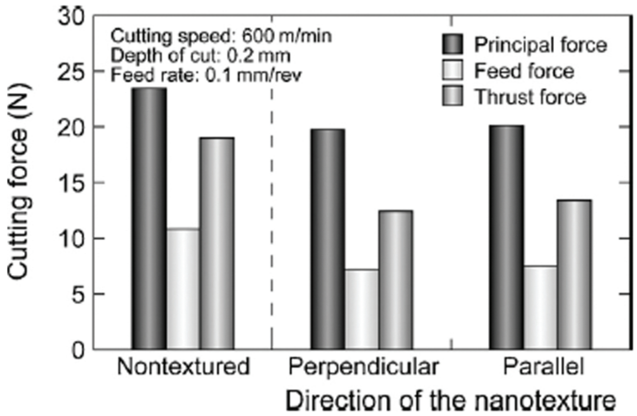

Figure 10. Comparison of the cutting forces required for the nanotextured tools with various texture directions [32].

Using cutting fluids is one of the effective methods to alleviate the severe friction and wear conditions in metal cutting operations. However, the lubrication effectiveness of cutting fluids reduces because of its difficult infiltration into the tool-chip interface during high-speed machining. Moreover, most of the fluids with environmentally harmful compositions are hard to dispose and expensive to recycle. Based on the above reasons, research on metal machining under dry condition has caused more attention for its positive role in reducing environment pollution and production costs. When machining under dry condition, the friction and adhesion between the chip and tool becomes higher, resulting in higher temperature and wear rates. It was thought that a solution to these problems could be achieved by developing new cutting tools with the purpose of reducing the heat generated by lowering the friction. In view of the above, nanoscale surface texturing was made on the rake face of the cutting tools with femtosecond laser pulses, which are expected to decrease friction and wear due to the reduced contact length at the tool-chip interface of the nanotextured tools. Deng et al. [34] fabricated nanoscale surface textures on the rake face close to the main cutting edge of the WC/TiC/Co carbide tools by femtosecond laser surface texturing. Dry cutting texts were carried out with the rake face-textured tools (TT) and the conventional carbide tools (CT). Results indicate that the cutting forces, the cutting temperature and the friction coefficient at the tool-chip interface of the TT were significantly reduced in comparison with that of the conventional CT:

$$F_f = a_w l_f \tau_c \tag{6}$$

where a_w is the cut width, l_f is the tool-chip contact length, and τ_c is the shear strength at the tool-chip interface, respectively. As shown in **Figure 11**, the nanoscale surface textures decrease the tool-chip contact length l_f, which result in the reduction of friction between the tool-chip interfaces.

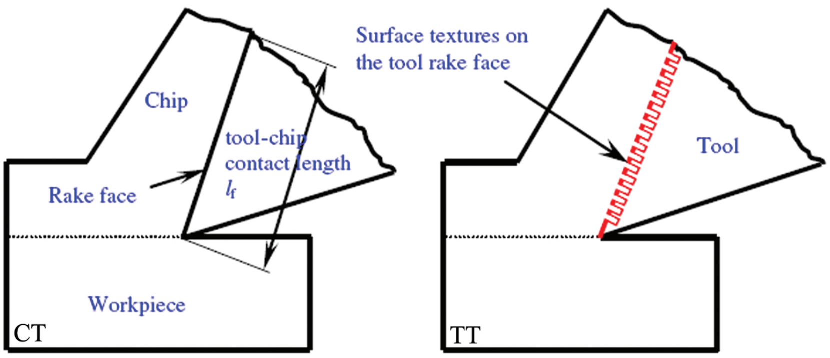

Figure 11. Schematic diagram of the tool-chip contact length for CT and TT. In the case of dry cutting, the friction force (Ff) at tool rake face can be calculated as [34].

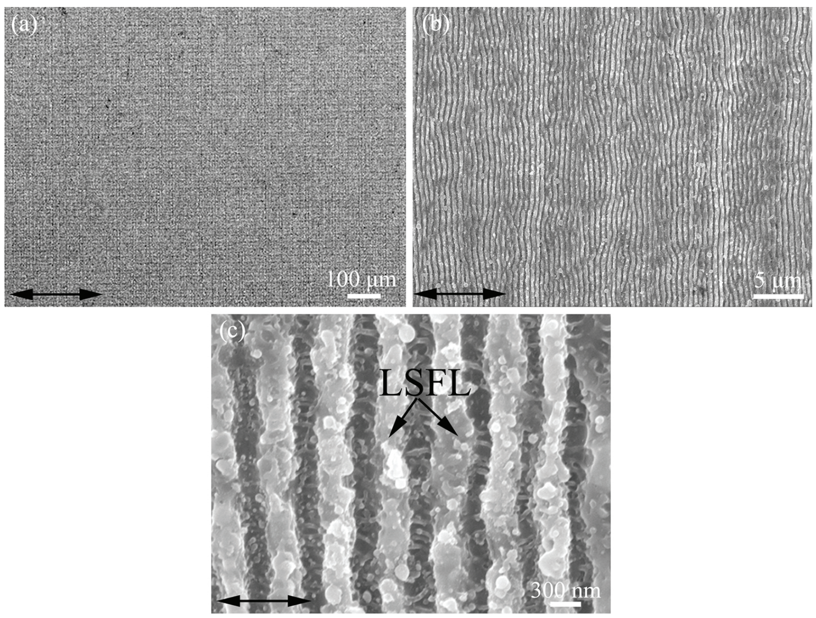

Figure 12. SEM micrographs of the LIPSS (laser-induced periodic surface structures) on the AISI 304L steel surfaces. Note the different magnifications used in (a)–(c). The black double-headed arrow indicates the polarization direction of the femtosecond laser pulses [35].

The authors of this chapter also [35] found the effect of femtosecond-laser-induced periodic surface structures (LIPSS) on the tribological properties of stainless steel in the conditions of starved lubrication and in dry contacts, respectively. By utilizing an 800-nm femtosecond laser to produce uniform ripple structures on the stainless steel surface are shown in **Figure 12**. The tribological properties of original surface and nanotextured surfaces with LIPSS were investigated under both dry and starved oil lubricated conditions. The friction coefficient of nanotextured surfaces with LIPSS has shown a lower value than that of the original surface under both dry and starved oil lubricated conditions. This finding may suggest applications in field such as microelectro-mechanical systems.

5. Manipulation of tribological properties of metals by ultrashort pulsed laser texturing and quenching

In the past, several classes of tribological experiments were developed in order to investigate the benefits of laser surface texturing in terms of transition between different lubrication regimes, reduction of friction coefficients, and reduction of wear rates. As a matter of fact, there exist possible local quenched effects accompanying with laser surface texturing process as a consequence of the interaction between laser beam and metal materials. As mentioned in Section 2, the time scale for a considerable energy transfer from electronics to the lattice is about 1 ps (10^{-12} s) during the interaction of pulse laser radiation with metal targets [41]. Thus, the thermal diffusivity cannot be neglected during the nanosecond or picosecond laser surface texturing process. The high energy deposited only in a very thin layer within picosecond time scale will result in the formation of a laser quenched layer on the textured surfaces. The laser quenching effects can lead to a reduction in grain size, phase transition, and change surface chemistry, which are possible to enhance tribological properties [59, 60].

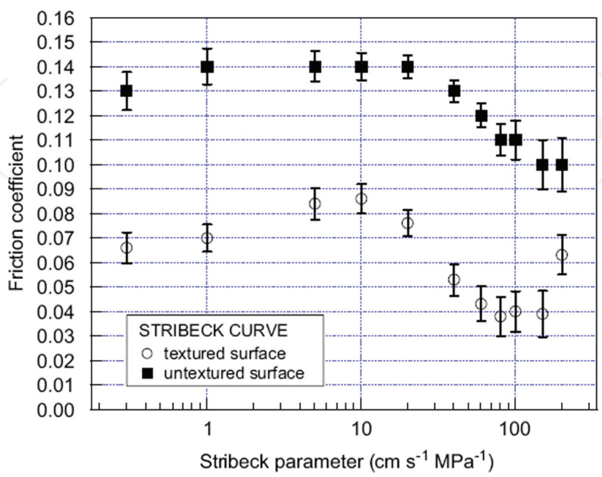

Figure 13. Friction coefficients against Stribeck parameters calculated as the ratio between mating speeds (range from 0.06 to 40 cm/s) and nominal contact pressures (maintained constant: roughly 0.2 MPa) [59].

Gualtieri et al. [59] fabricated microdimples on the 30NiCrMo12 nitride steel by nanosecond laser surface texturing. They also found that laser ablation in creating microdimples is accompanied to local quenching which caused grains size reduction and local hardening in micrometric subsurface areas near the microdimple edges. Tribological tests showed a reduction of friction coefficient due to the well-known hydrodynamic lift effect ensured by microdimples in full lubrication configuration (**Figure 13**). The local hardening induced by laser quenching may significantly improve the wear resistance of nitride steel during friction process.

Laser interference metallurgy is one possible approach to create well-defined surface topographies on the microscale accompanied with metallurgical effects including melting, resolidification, and the formation of intermetallic phases. Gachot et al. [60] applied the aforementioned technique to pattern both interacting surfaces (steel substrate and tribometer ball) to control the involved contact geometries under dry condition. They found that the dry friction between two laser-structured solids depends not only on the geometric characteristics of textured patterns but also on the surface chemistry and mechanical properties of textured surfaces.

Figure 14 shows the change of average friction coefficients of textured surfaces with different spacing in the process of picosecond laser surface texturing under dry condition. It can be seen that the average friction coefficients initially increase then decrease as the spacing of the microgroove increases. Moreover, the picosecond laser surface texturing can reduce the average friction coefficient if the microgrooves are distributed in an appropriate manner. The well-controlled tribological properties are attributed to the combined effects of laser surface texturing and laser quenching [61].

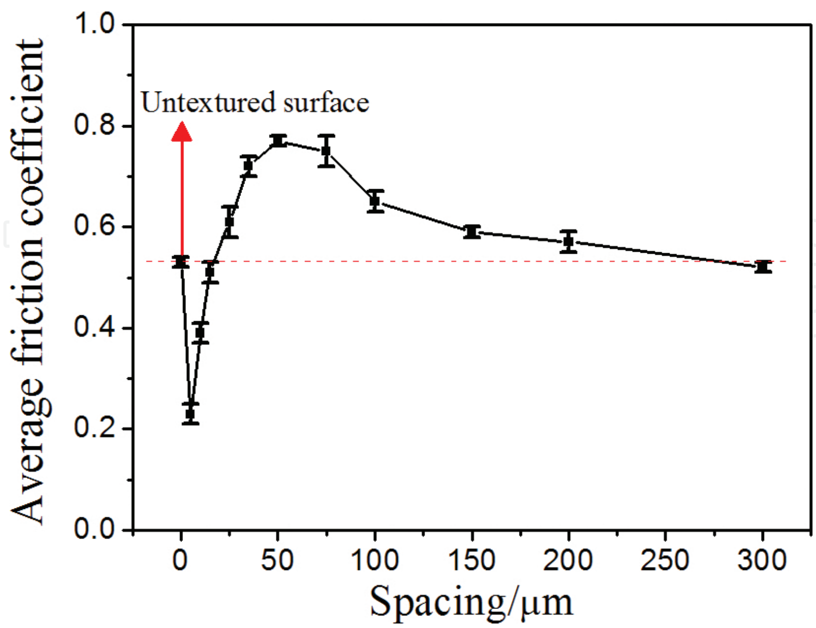

Figure 14. Average friction coefficients of untextured and textured surfaces with different spacing under dry condition [61].

6. Reduction of friction of metals by combining laser-induced periodic surface nanostructures and coating techniques

As mentioned above, laser-induced periodic surface nanostructures have marked potential to improve tribological properties of metal materials. However, only laser surface-texturing technology cannot meet strict requirements under harsh condition. As well known, coating materials surfaces with hard or soft solid lubricant has been considered to be a feasible method to enhance the tribological properties of materials. Thus, a combination of laser surface texturing and solid lubricating coatings are expected to significantly enhance the tribological properties of material substrates.

Lian et al. [36] developed an effective cutting tool named tungsten disulfide (WS_2) soft-coated nanotextured self-lubricating tool which is fabricated by two steps. First, nanoscale surface textures were produced on the tool-chip interface of rake face of uncoated YS8 (WC + TiC + Co) cemented carbide cutting inserts by femtosecond laser surface texturing. Then the nanotextured tools were deposited with WS_2 soft coatings by medium-frequency magnetron sputtering, multiarc ion plating, and ion beam-assisted deposition technique. From **Figure 15**, it can be seen that the friction coefficient at the tool-chip interface of the nanotextured tools (CFT) was reduced compared with that of the conventional one (YS8). Moreover, the WS_2 soft-coated nanotextured self-lubricating tool (CFTWS) exhibits the lowest friction coefficient among all the tools under the same tested condition. Zhang et al. [37] also studied the synergic effect of the laser-induced periodic surface nanostructures and the $Ti_{55}Al_{45}N$ hard coating on dry cutting property of WC/Co cutting tool. They developed two kinds of WC/Co-based $Ti_{55}Al_{45}N$ coated tools by changing processing sequence of femtosecond laser surface texturing and physical vapor deposition method as shown in **Figure 16**. Both the first $Ti_{55}Al_{45}N$-coated and then nanoscale-textured tools (CNT) and the first nanoscale-textured and then $Ti_{55}Al_{45}N$-coated tools (NCT) have lower friction coefficient compared with the conventional coated tool (CCT).

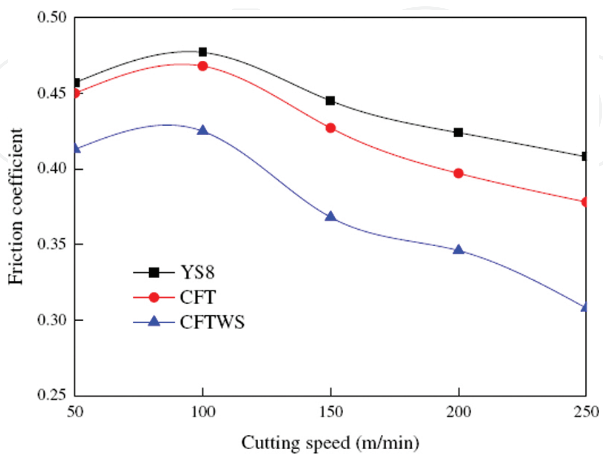

Figure 15. Friction coefficient between the tool-chip interface of the YS8, CFT, and CFTWS tools at different cutting speed (ap = 0.3 mm, f = 0.1 mm/r) [36].

http://dx.doi.org/10.5772/64764

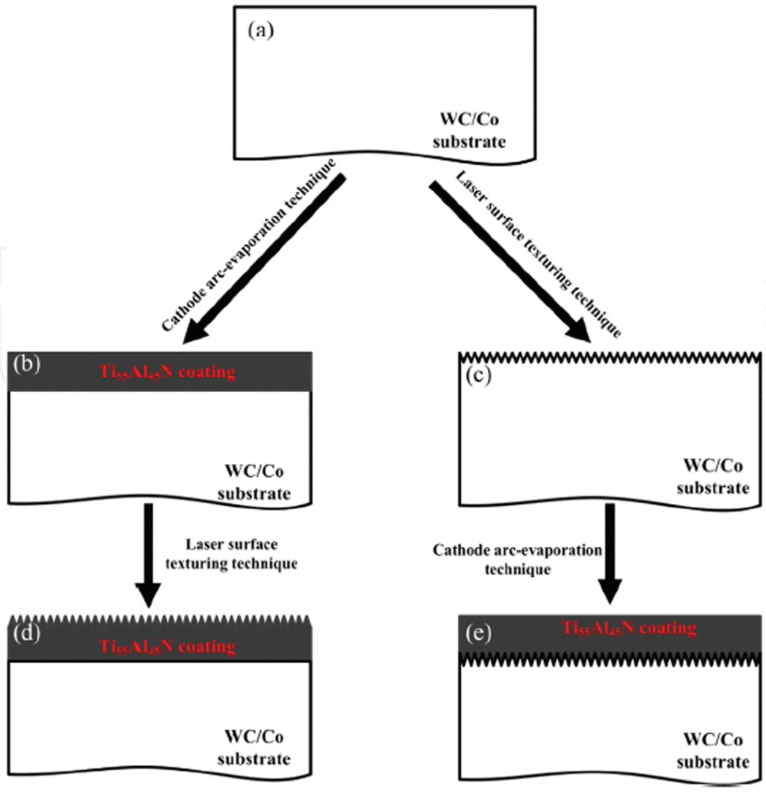

Figure 16. Schematic diagram showing the surface treatment procedure on WC/Co cemented carbide substrate: (a) polished, (b) coated, (c) textured, (d) first coated and then textured, and (e) first textured and then coated specimens [37].

7. Summary and outlook

There is an increasing need to control friction and wear in order to extend the lifetime of mechanical systems, to improve their reliability, and to conserve resources and energy. Previous investigations and applications have been demonstrated that tribological properties of metal materials can be improved by surface-texturing technology. However, ultrashort pulsed laser technology is considered as one of the most promising ways to achieve micromachining in the field of tribological applications, which is owing to its ultrashort pulse width and ultrahigh peak power that can process almost all materials. Moreover, ultrashort pulsed lasers are expected to minimize the heat-affected effects for surface texturing in tribological applications. To meet different requirements, various micro-/nanostructures can be produced by ultrashort pulsed laser surface texturing on the material surfaces to tune their tribological properties. Combining LIPSS with some solid lubricant coatings is also a good idea to obtain a desired reduction in friction and wear. What needs illustrating is that the surface textures are a kind of hierarchical structures consisting of micro-/nanostructures in the real application. Sugihara et al. [62] developed a cutting tool with a banded nano-/microtextured surface and it was revealed that the surface significantly improved the antiadhesiveness and lubricity. In a word, ultrashort pulsed laser surface texturing has a marked potential to modulate tribological properties of metal materials.

Author details

Quan-Zhong Zhao[1*] and Zhuo Wang[2]

*Address all correspondence to: zqz@siom.ac.cn

1 State Key Laboratory of High Field Laser Physics, Shanghai Institute of Optics and Fine Mechanics, Chinese Academy of Sciences, Shanghai, China

2 School of Materials Science and Engineering, Shanghai Jiao Tong University, Shanghai, China

References

[1] Etsion I. State of the art in laser surface texturing. J. Tribol-T. ASME. 2005; 127(1): 248–253. DOI: 10.1115/1.1828070

[2] Han Z, Zhang YS, Lu K. Friction and wear behavior of nanostructured metals. J. Mater. Sci. Technol. 2008; 24(4): 483–494.

[3] Fox-Rabinovich GS, Yamamoto K, Beake BD, Gershman IS, Kovalev AI, Veldhuis SC, Aguirre MH, Dosbaeva G, Endrino JL. Hierarchical adaptive nanostructured PVD coatings for extreme tribological applications: the quest for nonequilibrium states and emergent behavior. Sci. Technol. Adv. Mat. 2012; 13(4): 1–26. DOI: 10.1088/1468-6996/13/4/043001

[4] Vihena LM, Sedlacek M, Podgornik B. Surface texturing by pulsed Nd: YAG laser. Tribol. Int. 2009; 42(10): 1496–1504. DOI: 10.1016/j.triboint.2009.06.003

[5] Xing YQ, Deng JX, Wu Z, Cheng HW. Effect of regular surface textures generated by laser on tribological behavior of Si3N4/TiC ceramic. Appl. Surf. Sci. 2013; 265: 823–832. DOI: 10.1016/j.apsusc.2012.11.127

[6] Li KM, Yao ZQ, Hu YX, Gu WB. Friction and wear performance of laser peen textured surface under starved lubrication. Tribol. Int. 2014; 77: 97–105. DOI: 10.1016/j.triboint.2014.04.017

[7] Kovalchenko A, Ajayi O, Erdemir A, Fenske G, Etsion I. The effect of laser texturing of steel surfaces and speed-load parameters on the transition of lubrication regime from boundary to hydrodynamic. Tribol. Trans. 2004; 47(2): 299–307. DOI: 10.1080/05698190490440902

[8] Costa HL, Hutchings IM. Hydrodynamic lubrication of textured steel surfaces under reciprocating sliding conditions. Tribol. Int. 2007; 40(8): 1227–1238. DOI: 10.1016/j.triboint.2007.01.014

[9] Qiu Y, Khonsari MM. Experimental investigation of tribological performance of laser textured stainless steel rings. Tribol. Int. 2011; 44(5): 635–644. DOI: 10.1016/j.triboint.2011.01.003

[10] Ryk G, Etsion I. Testing piston rings with partial laser surface texturing for friction reduction. Wear. 2006; 261(7–8): 792–796. DOI: 10.1016/j.wear.2006.01.031

[11] Marian VG, Gabriel D, Knoll G, Filippone S. Theoretical and experimental analysis of a laser textured thrust bearing. Tribol. Lett. 2011; 44(3): 335–343. DOI: 10.1007/s11249-011-9857-8

[12] Wu Z, Deng JX, Chen Y, Xing YQ, Zhao J. Performance of the self-lubricating textured tools in dry cutting of Ti-6Al-4V. Int. J. Adv. Manuf. Tech. 2012, 62(9–12): 943–951. DOI: 10.1007/s00170-011-3853-x

[13] Raeymaekers B, Etsion I, Talke FE. Enhancing tribological performance of the magnetic tape/guide interface by laser surface texturing. Tribol. Lett. 2007; 27(1): 89–95. DOI: 10.1007/s11249-007-9211-3

[14] Komvopoulos K. Adhesion and friction forces in microelectromechanical system: mechanisms, measurement, surface medication techniques, and adhesion theory. J. Adhes. Sci. Technol. 2003; 17(4): 477–517. DOI: 10.1163/15685610360554384

[15] Pettersson U, Jacobson S. Textured surfaces for improved lubrication at high pressure and low sliding speed of roller/piston in hydraulic motors. Tribol. Int. 2007; 40(2): 355–359. DOI: 10.1016/j.triboint.2005.11.024

[16] Pettersson U, Jacobson S. Influence of surface texture on boundary lubricated sliding contacts. Tribol. Int. 2003; 36(11): 857–864. DOI: 10.1016/S0301-679X(03)00104-X

[17] Wang X, Kato K. Improving the anti-seizure ability of SiC seal in water with RIE texturing. Tribol. Lett. 2002; 14(4): 275–280. DOI: 10.1023/A:1022650813314

[18] He DQ, Zheng SX, Pu JB, Zhang GG, Hu LT. Improving tribological properties of titanium alloys by combining laser surface texturing and diamond-like carbon film. Tribol. Int. 2015; 82: 20–27. DOI: 10.1016/j.triboint.2014.09.017

[19] Chen CY, Wu BH, Chung CJ, Li WL, Chien CW, Wu PH, Cheng CW. Low-friction characteristics of nanostructured surfaces on silicon carbide for water-lubricated seals. Tribol. Lett. 2013; 51(1): 127–133. DOI: 10.1007/s11249-013-0153-7

[20] Chen CY, Chung CJ, Wu BH, Li WL, Chien CW, Wu PH, Cheng CW. Microstructure and lubricating property of ultra-fast pulse textured silicon carbide seals. Appl. Phys. A-Mater. 2012; 107(2): 345–350. DOI: 10.1007/s00339-012-6822-9

[21] Kietzig AM, Hatzikiriakos SG, Englezos P. Ice friction: the effects of surface roughness, structure, and hydrophobicity. J. Appl. Phys. 2009; 106(2): 0243031–0243037. DOI: 10.1063/1.3173346

[22] Sakai T, Nedyalkov N, Obara M. Friction characteristics of submicrometre-structured surfaces fabricated by particle-assisted near-field enhancement with femtosecond laser. J. Phys. D-Appl. Phys. 2007; 40(23): 7485–7491. DOI: 10.1088/0022-3727/40/23/035

[23] Garrelie F, Loir AS, Donnet LC, Rogemond F, Le Harzic R, Belin M, Audouard E, Laporte P. Femtosecond pulsed laser deposition of diamond-like carbon thin films for tribological application. Surf. Coat. Tech. 2003; 163: 306–312. DOI: 10.1016/S0257-8972(02)00481-4

[24] Arslan A, Masjuki HH, Varman M, Kalam MA, Quazi MM, Al Mahmud KAH, Gulzar M, Habibullah M. Effect of texture diameter and depth on the tribological performance of DLC coating under lubricated sliding condition. Appl. Surf. Sci. 2015; 356: 1135–1149. DOI: 10.1016/j.apsusc.2015.08.194

[25] Dumitru G, Romano V, Weber HP, Gerbig Y, Haefke H, Bruneau S, Hermann J, Sentis M. Femtosecond laser ablation of cemented carbides: properties and tribological applications. Appl. Phys. A-Mater. 2004; 79(3): 629–632. DOI: 10.1007/s00339-004-2675-1

[26] Bathe R, Krishna VS, Nikumb SK, Padmanabham G. Laser surface texturing of gray cast iron for improving tribological behavior. Appl. Phys. A-Mater. 2014; 117(1): 117–123. DOI: 10.1007/s00339-014-8281-y

[27] Wang Z, Zhao QZ, Wang CW, Zhang Y. Modulation of dry tribological property of stainless steel by femtosecond laser surface texturing. Appl. Phys. A-Mater. 2015; 119(3): 1155–1163. DOI: 10.1007/s00339-015-9085-4

[28] Lei ST, Devarajan S, Chang ZH. A study of micropool lubricated cutting tool in machining of mild steel. J. Mater. Process. Tech. 2009; 209(3): 1612–1620. DOI: 10.1016/j.jmatprotec.2008.04.024

[29] Ling TD, Liu PZ, Xiong SW, Grzina D, Cao J, Wang QJ, Xia ZC, Talwar R. Surface texturing of drill bits for adhesion reduction and tool life enhancement. Tribol. Lett. 2013; 52(1): 113–122. DOI: 10.1007/s11249-013-0198-7

[30] Wang Z, Li YB, Bai F, Wang CW, Zhao QZ. Angle-dependent lubricated tribological properties of stainless steel by femtosecond laser surface texturing. Opt. Laser Technol. 2016; 81: 60–66. DOI:10.1016/j.optlastec.2016.01.034

[31] Tagawa N, Takada M, Mori A, Sawada H, Kawahara K. Development of contact sliders with nanotextures by femtosecond laser processing. Tribol. Lett. 2006; 24(2): 143–149. DOI: 10.1007/s11249-006-9142-4

[32] Kawasegi N, Sugimori H, Morimoto H, Morita N, Hori I. Development of cutting tools with microscale and nanoscale textures to improve frictional behavior. Precis. Eng. 2009; 33(3): 248–254. DOI: 10.1016/j.precisioneng.2008.07.005

[33] Zhang KD, Deng JX, Sun JL, Jiang C, Liu YY, Chen SA. Effect of micro/nano-scale textures on anti-adhesive wear properties of WC/Co-based TiAlN coated tools in AISI

316 austenitic stainless steel cutting. Appl. Surf. Sci. 2015; 335: 602–614. DOI: 10.1016/j.apsusc.2015.07.132

[34] Deng JX, Lian YS, Wu Z, Xing YQ. Performance of femtosecond laser-textured cutting tools deposited with WS2 solid lubricant coatings. Surf. Coat. Tech. 2013; 222: 135–143. DOI: 10.1016/j.surfcoat.2013.02.015

[35] Wang Z, Zhao QZ, Wang CW. Reduction of friction of metals using laser-induced periodic surface nanostructures. Micromachines 2015; 6(11): 1606–1616. DOI: 10.3390/mi6111444

[36] Lian YS, Deng JX, Yan GY, Cheng HW, Zhao J. Preparation of tungsten disulfide (WS2) soft-coated nano-textured self-lubricating tool and its cutting performance. Int. J. Adv. Manuf. Tech. 2013; 68(9–12): 2033–2042. DOI: 10.1007/s00170-013-4827-y

[37] Zhang KD, Deng JX, Meng R, Gao P, Yue HZ. Effect of nano-scale textures on cutting performance of WC/Co-based Ti55Al45N coated tools in dry cutting. Int. J. Refract. Met. H. 2015; 51: 35–49. DOI: 10.1016/j.ijrmhm.2015.02.011

[38] Von der linde D, Sokolowski-Tinten, K, Bialkowski J. Laser-solid interaction in the femtosecond time regime. Appl. Surf. Sci. 1997; 109: 1–10. DOI: 10.1016/S0169-4332(96)00611-3

[39] Momma C, Nolte S, Chichkov BN, Alvensleben FV, Tunnermann A. Precise laser ablation with ultrashort pulses. Appl. Surf. Sci. 1997; 109: 15–19. DOI: 10.1016/S0169-4332(96)00613-7

[40] Becker PC, Fragnito HL, Brito Cruz CH, Fork RL, Cunningham JE, Henry JE, Shank CV. Femtosecond photon echoes from band-to-band transitions in GaAs. Phys. Rev. Lett. 1988; 61(14): 1647–1649. DOI: 10.1103/PhysRevLett.61.1647

[41] Chichkov BN, Momma C, Nolte S, Alvensleben FV, Tunnermann A. Femtosecond, picosecond and nanosecond laser ablation of solids. Appl. Phys. A-Mater. 1996; 63(2): 109–115.

[42] Birnbaum M. Semiconductor surface damage produced by ruby lasers. J. Appl. Phys. 1965; 36: 3688–3689.

[43] Wu B, Zhou M, Li J, Ye X, Li G, Cai L. Superhydrophobic surfaces fabricated by microstructuring of stainless steel using a femtosecond laser. Appl. Surf. Sci. 2009; 256(1): 61–66. DOI: 10.1016/j.apsusc.2009.07.061

[44] Ahsan MS, Ahmed F, Kim YG, Lee MS, Jun MBG. Colorizing stainless steel surface by femtosecond laser induced micro/nano-structures. Appl. Surf. Sci. 2011; 257(17): 7771–7777. DOI: 10.1016/j.apsusc.2011.04.027

[45] Yasumaru N, Miyazaki K, Kiuchi J. Control of tribological properties of diamond-like carbon films with femtosecond-laser-induced nanostructuring. Appl. Surf. Sci. 2008; 254(8): 2364–2368. DOI: 10.1016/j.apsusc.2007.09.037

[46] Zhao QZ, Malzer S, Wang LJ. Formation of subwavelength periodic structures on tungsten induced by ultrashort laser pulses. Opt. Lett. 2007; 32(3): 1932–1934. DOI: 10.1364/OL.32.001932

[47] Mannion PT, Magee J, Coyne E, O'Connor GM, Glynn TJ. The effect of damage accumulation behavior on ablation thresholds and damage morphology in ultrafast laser micro-machining of common metals in air. Appl. Surf. Sci. 2004; 233(1–4): 275–287. DOI: 10.1016/j.apsusc.2004.03.229

[48] Yasumaru N, Sentoku E, Miyazaki K, Kiuchi J. Femtosecond-laser-induced nanostructure formed on nitride stainless steel. Appl. Surf. Sci. 2013; 264(12): 611–615. DOI: 10.1016/j.apsusc.2012.10.076

[49] Bizi-bandoki P, Valette S, Audouard E, Benayoun S. Effect of stationary femtosecond laser irradiation on substructures' formation on a mold stainless steel surface. Appl. Surf. Sci. 2013; 270: 197–204. DOI: 10.1016/j.apsusc.2012.12.168

[50] Huang M, Zhao FL, Cheng Y, Xu NS, Xu ZZ. Origin of laser-induced near-subwavelength ripples: interference between surface plasmons and incident laser. ACS Nano 2009; 3(12): 4062–4070. DOI: 10.1021/nn900654v

[51] Buividas R, Mikutis M, Juodkazis S. Surface and bulk structuring of materials by ripples with long and short laser pulses: recent advances. Prog. Quant. Electron. 2014; 38(3): 119–156. DOI: 10.1016/j.pquantelec.2014.03.002

[52] Zhou GS, Fauchet PM, Siegman AE. Growth of spontaneous periodic surface structures on solids during laser illumination. Phys. Rev. B 1982; 26(10): 5366–5381. DOI: 10.1103/PhysRevB.26.5366

[53] Soileau MJ. Ripple structures associated with ordered surface defects in dielectrics. IEEE J. Quantum Elect. 1984; 20(5): 464–467. DOI: 10.1109/JQE.1984.1072422

[54] Emmony DC, Howson RP, Willis LJ. Laser mirror damage in germanium at 10.6 μm. Appl. Phys. Lett. 1973; 23(11): 598–600. DOI: 10.1063/1.1654761

[55] Raether H. Surface plasmons on smooth and rough surfaces and on gratings. Springer; 1988. DOI: 10.1007/BFb0048317

[56] Suh NP, Sin HC. The genesis of friction. Wear 1981; 69(1): 91–114. DOI: 10.1016/0043-1648(81)90315-X

[57] Kim DE, Suh NP. On microscopic mechanism of friction and wear. Wear 1991; 149(1–2): 199–208. DOI:10.1016/0043-1648(91)90373-3

[58] Ding Q, Wang LP, Hu LT, Hu TC, Wang Y. The pairing-dependent effects of laser surface texturing on micro tribological behavior of amorphous carbon film. Wear 2012; 274: 43–49. DOI: 10.1016/j.wear.2011.08.008

[59] Gualtieri E, Borghi A, Calabri L, Pugno N, Valeri S. Increasing nanohardness and reducing friction of nitride steel by laser surface texturing. Tribol. Int. 2009; 42(5): 699–705. DOI: 10.1016/j.triboint.2008.09.008

[60] Gachot C, Rosenkranz A, Reinert L, Ramos-Moore E, Souza N, Muser MH, Mucklich F. Dry friction between laser-patterned surfaces: role of alignment, structural wavelength and surface chemistry. Tribol. Lett. 2013; 49(1): 193–202. DOI: 10.1007/s11249-012-0057-y

[61] Wang Z, Wang CW, Wang M, Zhao QZ. Manipulation of tribological properties of stainless steel by picosecond laser texturing and quenching. To be published on Tribol. Int.

[62] Sugihara T, Enomoto T. Development of a cutting tool with a nano/micro-textured surface-improvement of anti-adhesive effects by considering the texture patterns. Precis. Eng. 2009; 33(4): 425–429. DOI: 10.1016/j.precisioneng.2008.11.004

IntechOpen